Cooling and Heating a Greenhouse in Baghdad by a Solar Assisted Desiccant System

Prof. Dr. Khalid Ahmed Joudi
Department of Mechanical Engineering
University of Baghdad
E-mail: khalid47joudi@yahoo.com

Mustafa Moayad Hasan
Department of Mechanical Engineering
University of Baghdad
E-mail: mustafa_h1987@yahoo.com

ABSTRACT

Modeling the microclimate of a greenhouse located in Baghdad under its weather conditions to calculate the heating and cooling loads by computer simulation. Solar collectors with a V-corrugated absorber plate and an auxiliary heat source were used as a heating system. A rotary silica gel desiccant dehumidifier, a sensible heat exchanger, and an evaporative cooler were added to the collectors to form an open-cycle solar assisted desiccant cooling system. A dynamic model was adopted to predict the inside air and the soil surface temperatures of the greenhouse. These temperatures are used to predict the greenhouse heating and cooling loads through an energy balance method which takes into account the soil heat gain. This is not included in conventional methods. The results showed satisfactory agreement with published papers. Also, the results of heating and cooling loads obtained revealed good agreement with those obtained from conventional methods when the soil heat gain is included. Two identical collectors in series of total area of 5.4m^2 were employed as a heating system which provides an outlet air temperature of 30 ^{o}C at air mass flux of 0.06 kg/s.m^2 at midday in January. While, a 65 ^{o}C outlet air temperature was achieved for the same mass flux at midday in August. The desiccant cooling system was operated in five operating modes; the ventilation mode and four recirculation modes with 20%, 50%, 70%, and 90% recirculation. The simulation results showed that a regeneration temperature of 60-70 ^{o}C is satisfactory for a cool supply air temperature of about 19.5 ^{o}C. Also, it was noted that 20-30 % recirculation of return air would result in suitable indoor greenhouse conditions for most periods of system operation. In addition, the coefficient of performance COP of the system was high compared with the conventional vapor compression systems.

KEYWORDS: Solar cooling & heating; Greenhouse microclimate; Greenhouse heating/ Cooling loads; Soil heat gain; Solid desiccant system; Computer simulation;

تبريد وتدفئة بيت زجاجي في بغداد بأستخدام منظومة امتزازية تعمل بمساعدة الطاقة الشمسية

أ.د خالد أحمد الجودي
قسم الهندسة الميكانيكية
جامعة بغداد

مصطفى مؤيد حسن
قسم الهندسة الميكانيكية
جامعة بغداد

الخلاصه

يُعنى هذا البحث بنمذجة البيئه الداخلية لبيت زجاجي في بغداد وتحت ظروفها المناخية الحقيقية لحساب حملي التدفئه والتبريد بأستخدام تقنيه الحاسوب. مجمعات شمسيه ذات صفيحة امتصاص مضلعه ومصدر حراري مساعد استخدمت كمنظومة تدفئة مع قرص تجفيف دوار محشو بمادة تجفيفيه هي السيليكاجيل ومبادل حراري لأنتزاع الحرارة المحسوسه ومبرد تبخيري الى منظومة التدفئه لتكوين منظومة تبريد امتزازيه مفتوحه تعمل بمساعدة الطاقه الشمسيه. استخدمت النمذجة الديناميكية للتنبؤ بدرجتي حرارة هواء البيت الزجاجي وسطح تربته إذ تعد هاتين الدرجتين اساسيتين في حساب حملي التدفئه والتبريد للبيت الزجاجي بطريقة توازن الطاقه. هذه الطريقة وبخلاف الطرق التقليديه المتبعه تأخذ بنظر الأعتبار الكسب الحراري من سطح التربه. أظهرت النتائج تقارباً واضحاً مع نتائج نماذج أُخرى لبحوث منشورة. كما ان أحمال التدفئة والتبريد التي حسبت كانت متطابقة مع

نتائج الطرق التقليديه عند اضافة الكسب الحراري من التربة الى تلك الطرق. اقتصرت منظومة التدفئة على زوج متماثل من المجمعات بمساحة كلية 5.4 م^2 والتي أعطت هواء بدرجة حرارة 30 ^{o}م وبمعدل تدفق 0,06 كغم/ثا لكل متر مربع من مساحة المجمع في منتصف النهار في شهر كانون الثاني. بينما تم الحصول على هواء بدرجة حرارة 65 ^{o}م ولمعدل التدفق نفسه في منتصف النهار في شهر آب.تم تشغيل منظومة التبريد الأمتزازيه بخمس طرق تشغيل وهي نمط التهويه واربع انماط من اعادة التدوير; 20%، 50%، 70%، و 90% من الهواء الراجع. وقد أظهرت نتائج محاكاة المنظومه بأن درجة حرارة اعادة النتشيط بين 60-70 ^{o} م تعطي نتائج أفضل من حيث درجة حرارة تجهيز الهواء والتي بلغت تقريباً 19.5 ^{o} م عندما كانت الظروف الداخليه 28 ^{o} م و رطوبه نسبيه 70%. كذلك فأن تشغيل المنظومه مع تدوير الهواء الراجع بنسبة 20-30% يوفر ظروف ملائمه داخل البيت الزجاجي ولمعظم ساعات التشغيل. وجد ايضاً أن معامل أداء منظومة التبريد الامتزازيه عالي جداً مقارنة بأجهزة تكييف الهواء الأنضغاطية.

الكلمات الرئيسية: تبريد وتدفئة شمسية لبيت زجاجي; البيئة الدقيقة لبيت زجاجي; أحمال التبريد/التدفئة لبيت زجاجي; كسب تربة حراري; منظومة امتزاز صلبة; تقنية الحاسوب.

1. INTRODUCTION

A greenhouse is an enclosed structure covered with transparent material that utilizes solar radiant energy to grow plants in or outside the cultivation season. A brief description about greenhouses is given by Mastalerz 1977 and, Aldrich and Bartok 1994.

The assemblage of environmental factors surrounding living plants in a greenhouse is termed as greenhouse microclimate. It may be affected by the orientation of the greenhouse, latitude, area of the greenhouse, plant canopy area, bare soil surface area, structural design, properties of the greenhouse construction material, etc. A greenhouse model is a mathematically simplified representation of a very complicated real system. The models are usually in forms of computer programs and can be classified either as static or dynamic models (Kano 1985).

The initial work of static or steady-state models was done by Businger 1963. These models are less accurate due to their simplicity and involve only few parameters. Further, they cannot account for the storage of heat.

Dynamic models are important for simulating the greenhouse response on a small timescale. Singh et al. 2006 developed a mathematical model using a computer program written in C^{++} language to model the microclimate of a semi-quonset type greenhouse. It was solved using Gauss–Seidal iteration method under appropriate assumptions and inputs. The results were compared with the experimental data and agreement was found. Rodriguez et al. 2010 developed an interactive dynamic greenhouse environment simulator. This model was implemented in a web-based interactive application that allowed for the selection of the greenhouse design, weather conditions, and operational strategies. The simulator produced realistic approximations of the dynamic behavior of greenhouse environments with different design configurations for 28-h simulation periods.

The existing heating systems for greenhouses are: water storage, rock bed storage, phase change material storage, movable insulation, ground air collector GAC, north wall storage, and mulching (Sethi and Sharma 2008). The heat storage medium can be placed inside the greenhouse on the path rows along the ground surface of a greenhouse near the plants, at the north side of the greenhouse or at the center of the greenhouse.

Pebble, gravel and bricks are the popular and economical solid heat storage materials. They store excess heat during the day and transfer it to the cool air at night. A rock-bed system by Kurklu et al. 2003 created an air temperature difference of about 10°C at night.

During night time in winter months, a thermal screen/curtain is rolled up during daytime to allow solar radiation for thermal heating (Sethi and Sharma 2008). Active solar heating systems for greenhouses are reviewed by Sethi and Sharma 2008.

The existing cooling technologies for greenhouses are: natural/mechanical ventilation, shading, and evaporative cooling. It has been found that the total area of vent openings should be 15-30% of floor area as further increase in vent openings gives marginal increase in performance (White and Aldrich 1975).

Current evaporative cooling methods are; fan-pad, fog/mist, and roof evaporative cooling systems. Fan-pad system consists of a fan on one sidewall and a wet pad on the other sidewall of the greenhouse. Jain and Tiwari 2002 conducted theoretical and experimental studies in a greenhouse with fan-pad evaporative cooling system. Greenhouse air temperature was reported 4–5^{o}C lower than the ambient temperature. They found that among the studied parameters, the length of the

greenhouse and the height of the cooling pad were sensitive to cooling more than the air mass flow rate. Shukla et al. 2008 saw that employing an inner thermal curtain makes the evaporative cooling more effective for the greenhouse. Davies 2005 reported a study where liquid desiccant along with solar regeneration was used to reduce the temperature inside a greenhouse having evaporative cooling system.

Fog/mist system is based on spraying the water as small droplets with high pressure into the air above the plants in order to increase the water surface in contact with the air and to create high relative humidity. The cooling efficiency of fogging system was investigated by Abdel-Ghany and Kozai 2006. The results showed that a fogging cycle of 60 s on, 180 s off provided a relatively higher value of efficiency than other cycles.

Recently, an earth to air heat exchanger system EAHES and aquifer coupled cavity flow heat exchanger system ACCFHES were successfully used (Sethi and Sharma 2008). They are known as composite systems and used the ground potential for greenhouse heating and cooling. EAHES basically consists of underground pipes and an airflow system, which forces the air through the pipes. Cold air from inside the greenhouse is circulated through the pipes. Heat is transferred from the soil to the air stream and then returned to the greenhouse. The same system can also be used for cooling during the summer conditions.

In the hottest region and when the above cooling techniques become ineffective, a refrigeration system is used, but such a system is characterized as a high operating cost system. Thus, alternatives to classical air-conditioners are in need. Among these alternatives, open-cycle desiccant cooling systems which are commonly called desiccant evaporative cooling systems. This system consists of solar air heater, rotating disk dehumidifier, heat exchanger and evaporative cooler. It could operate with two modes, ventilation and recirculation. Joudi and Madhi 1985 carried out tests at Basrah city, Iraq using solar energy for regeneration of the silica gel desiccant. Also, tests were carried out for constant regeneration temperature of 70^{o}C which is obtainable with air heating solar collectors. The system performance improved with higher regeneration temperature, higher process air mass flow rate and dry weather. Later on, Moneer 1997 and Joudi and Dhaidan 2001 evaluated the performance of the same desiccant cooling system under various design and operating parameters using computer simulation. They found that the ambient temperature, regeneration temperature, heat exchanger effectiveness and evaporative cooler effectiveness have major influence on the system performance, whereas the dehumidifier has a minor effect.

The present work attempts to model the inside microclimate of a stand alone, east-west orientation, gable shaped glasshouse without plants and located at Baghdad, Iraq (33.3^{o}N, 44.4^{o}E). The greenhouse was assumed to have dimensions of 4 m length, 2 m width and central height of 3m; 2 m to the eave and 1 m to the ridge. A simulation program was developed for the prediction of the microclimate employing a simple dynamic model based on an assumption that the greenhouse is a big solar collector with two main components. The air enclosed by the structure and the greenhouse soil. The soil thermal properties were assumed to be constant. This is quite different from other dynamic models cited in the literature. Also, the hourly heating and cooling loads were based on an energy balance method which include solar and soil heat gains that have not been taken into consideration in the literature.

2. PREDICTION OF THE GREENHOUSE MICROCLIMATE BY A DYNAMIC MODEL

The greenhouse under study is illustrated in **Fig. 1** with all the heat exchanges with the surroundings. The mathematical model consists of two first-order differential equations derived from an energy balance written for the inside air temperature and soil surface temperature under the following assumptions:

1. Storage capacity of the walls and the roof material was neglected.
2. The air and top soil temperatures are uniform.
3. No evaporation occurs from the soil.

The energy balance equation of the air enclosed by the greenhouse glazing, per m^2 of soil surface area, can be written as:

$$q_{sg} + q_g = \frac{dq_i}{dt} + q_t + q_{inf} \quad (1)$$

The energy balance of the bare soil per m^2 of soil surface area can be written as:

$$q_{ss} = \frac{dq_s}{dt} + q_g + q_k \quad (2)$$

The greenhouse soil is considered as a significant heat source which can compensate the energy losses through the walls especially during the night (Mesmoudi et al. 2010).

The rate of solar energy absorbed within the greenhouse air can be estimated as (Aldrich and Bartok 1994):

$$q_{sg} = \tau I_h \quad (3)$$

The rate of energy used to raise the inside air temperature and the soil surface temperature are given by Rodriguez et al. 2010 as:

$$\frac{dq_i}{dt} = \rho\, c_p\, H\, \frac{dT_i}{dt} \quad (4)$$

$$\frac{dq_s}{dt} = C_s\, z_o\, \frac{dT_s}{dt} \quad (5)$$

The rate of energy transferred from the soil surface to the interior air by convection ($q_{co.}$) and radiation (q_r) modes are given by Amri-Alm 1997 as:

$$q_g = q_{co.} + q_r \quad (6)$$

$$q_{co.} = h_s\,(T_s - T_i) \quad (7)$$

$$q_r = \epsilon_s\, \sigma\, \left(T_s^{\,4} - T_i^{\,4}\right) \quad (8)$$

The convection heat transfer coefficient between the bare soil surface and the interior air was estimated as (Roy et al. 2002):

$$h_s = 10\,(T_s - T_i)^{\,0.33} \quad (9)$$

The largest exchanges are by transmission and infiltration through the greenhouse cover:

$$q_t = U\, r\, (T_i - T_a) \quad (10)$$

$$q_{inf} = \rho\, c_p\, N\, H (T_i - T_a)/3600 \quad (11)$$

Rodriguez et al. 2010 calculated the conducted heat from the soil surface of zero depth z_o to the ground beneath at a certain depth z_b as:

$$q_k = \frac{k_s (T_s - T_b)}{(z_o + z_b)} \quad (12)$$

Thus, eqs. (1) and (2) become:

$$\frac{dT_i}{dt} = \frac{1}{\rho\, c_p\, H}\left[\tau\, I_h + h_s (T_s - T_i) + \epsilon_s\, \sigma\, \left(T_s^{\,4} - T_i^{\,4}\right) - U\, r\, (T_i - T_a) - \frac{\rho\, c_p\, N\, H\, (T_i - T_a)}{3600}\right] \quad (13)$$

$$\frac{dT_s}{dt} = \frac{1}{C_s\, z_o}\left[\alpha_s\, \tau\, I_h - h_s (T_s - T_i) - \epsilon_s \sigma (T_s^{\,4} - T_i^{\,4}) - \frac{k_s (T_s - T_b)}{(z_o + z_b)}\right] \quad (14)$$

Table 1 gives the constants used in eqs. (13) and (14) and a MATLAB standard solver (ode45) was used to solve theses equations numerically using a classical fourth-order Runge–Kutta method. The initial conditions for each of the state variables and for time (t = 0) were assumed to be ($T_i = T_a$) and ($T_s = T_a$).

3. ESTIMATING HEATING AND COOLING LOADS BY ENERGY BALANCE METHOD

Estimating the heating and cooling loads of a greenhouse includes conduction, infiltration, and ventilation energy exchange. In addition, the calculations must consider solar energy which is usually much greater for greenhouses than for conventional buildings. The greenhouse in the present work was considered as a solar collector having an absorber plate (i.e., the greenhouse soil). This concept was recently adopted by Aldrich and Bartok 1994, Abdel-Ghany and Al-Helal 2011, Abdel-Ghany 2011. An energy balance was adopted to estimate both the heating and cooling loads of the greenhouse. The energy balance equation includes the soil heat gain which has not been included by Mastalerz 1977, ASHRAE 1977, Aldrich and Bartok 1994. The energy needed to maintain the

inside temperature of the greenhouse at the favorable level can be written as (Hepbasli 2011):

$$\text{Energy needed} = \sum \text{Heat loss} - \sum \text{Heat gain} \quad (15)$$

3.1 Estimating The Heating Load

Calculating the heating load involves conduction through the structural cover plus infiltration of outdoor air, which are calculated using eqs. (10) & (11), respectively. The sources of heat gain of greenhouse comprise solar and soil gains. Thus, according to eq. (14), the heat load of the greenhouse will be:

$$\text{Heat load} = \left[U r + \rho\, c_p\, N \frac{H}{3600} \right] (T_d - T_a) - [\tau\, I_h + h_s (T_s - T_i) + \epsilon_s\, \sigma\, (T_s^{\,4} - T_i^{\,4})] \quad (16)$$

3.2 Estimating The Cooling Load

Calculating the cooling load involves the sum of heat gain sources to the interior of the greenhouse. Generally, the cooling load due to heat gain through fenestrations comprises two terms; the solar heat gain and the transmission heat gain due to temperature difference (ASHRAE 1977) as:

$$q = (SC \times SHG_{max} \times CLF) + (U \times CLTD) \quad (17)$$

Sethi and Sharma 2007 presented the concept of sol-air temperature for cooling load calculation. Sol–air temperature is interpreted as the temperature of the surroundings that will produce the same heating effect as the incident radiation in conjunction with the actual ambient air temperature. The sol-air temperature is calculated as:

$$T_{sa} = \frac{\tau\, I_h}{U} + T_a \quad (18)$$

Therefore, the heat gain in summer to be removed from the greenhouse is given as (Sethi and Sharma 2007):

$$q = U\,(T_{sa} - T_d) \quad (19)$$

As mentioned earlier in section 3, the heat gain in a greenhouse occurs due to soil, cover (by conduction and infiltration), and solar energy. Thus, the cooling load, in this work, will be taken as the sum of these heat gain sources:

$$\text{Cooling load} = \left[U r + \rho\, c_p\, N \frac{H}{3600} \right] (T_a - T_d) + \tau\, I_h + h_s (T_s - T_i) + \epsilon_s\, \sigma (T_s^{\,4} - T_i^{\,4}) \quad (20)$$

4. MODELING OF THE OPEN CYCLE DESICCANT COOLING SYSTEM

The cooling system employed in the present work consists of four major components. The rotary desiccant dehumidifier in which the adsorption/ desorption processes take place. V-corrugated solar air heaters as a heat source for the regeneration process. A water-cooled sensible heat exchanger and an evaporative cooler. A schematic diagram of the simulated system with its presentation on the psychometric chart is illustrated in **Fig. 2 a, b.** The mathematical models for each component of the system are presented in the following sections.

4.1 Solar Air Heater Model

At steady state, the useful energy gain of a collector is the difference between the absorbed solar radiation and the thermal losses (Duffie and Beckman 2006):

$$Q_u = A_c [S - U_l (T_p - T_a)] \quad (21)$$

Total collector area was 5.4 m^2 The absorbed solar energy by the collector S can be calculated on an hourly basis as (Duffie and Beckman 2006):

$$S = D_f\, .S_f\, [I_b (\tau\alpha)_{eb} + I_d (\tau\alpha)_{ed} + I_r (\tau\alpha)_{er}] \quad (22)$$

It is convenient to express the useful energy in terms of the inlet fluid temperature and a parameter called the collector heat removal factor. Therefore, the useful energy becomes:

$$Q_u = A_c F_R [S - U_l (T_i - T_a)] \quad (23)$$

A measure of collector performance is the collection efficiency which is defined as the ratio of

the useful gain over some specified time period to the incident solar energy over the same time period (Duffie and Beckman 2006):

$$\eta = \frac{Q_u}{A_c\, I_t} \tag{24}$$

The outlet air temperature from the solar air heater which is used as a regeneration temperature for the desorption process of the solid desiccant is calculated as (Duffie and Beckman 2006):

$$T_o = T_i + \frac{Q_u}{G\, c_p} \tag{25}$$

4.2 Desiccant Dehumidifier Analysis

The mathematical model of the desiccant wheel is basically represented by two isopotential lines $B1$ and $B2$ applied for the process air stream and the regeneration air stream respectively. They are defined by Fong et al. 2010 as:

$$B1 = \frac{-2865}{T^{1.49}} + 4.344\, w^{0.8624} \tag{26}$$

$$B2 = \frac{T^{1.49}}{6360} - 1.127\, w^{0.07969} \tag{27}$$

The above potentials for the inlet conditions of the process and regeneration air streams (temperature and moisture content) are easily estimated from the known conditions of the entering streams. Then, the combined potentials for the outlet process air stream are obtained from the following regenerative dehumidifier efficiencies (Joudi and Dhaidan 2001):

$$B1_{po} = \eta_{B1}\left(B1_{ri} - B1_{pi}\right) + B1_{pi} \tag{28}$$

$$B2_{po} = \eta_{B2}\left(B2_{ri} - B2_{pi}\right) + B2_{pi} \tag{29}$$

Where

$B1_{pi}$, $B2_{pi}$ = combined potentials for inlet process air stream.

$B1_{ri}$, $B2_{ri}$= combined potentials for inlet regeneration air stream.

$B1_{po}$, $B2_{po}$ = combined potentials for the outlet process air stream.

η_{B1} , η_{B2} = regenerative dehumidifier $B1$ and $B2$ potential efficiencies, respectively.

The outlet process air temperature and moisture content where obtained by solving eqs. (26) and (27) simultaneously with the combined potential calculated from eqs. (28) and (29),

respectively. Generally, there are three pairs of (η_{B1},η_{B2}) values. (0.05, 0.95), (0.08, 0.8), and (0.1, 0.7) which refer to good, medium, and poor dehumidifier performances respectively (Joudi and Dhaidan 2001). The values of (0.2, 0.55) were used in this work.

4.3 Sensible And Evaporative Cooler Effectiveness

After the dehumidification process, the outlet process air becomes hot and dry. Therefore, the air is sensibly cooled first by a heat exchanger. A water-cooled cross flow heat exchanger was assumed for this purpose. The outlet state of the process air from the heat exchanger is calculated using the usual heat exchanger effectiveness correlation given as:

$$T_{po} = T_{pi} + \varepsilon_{hx}\left(T_{wi} - T_{pi}\right) \tag{30}$$

The temperature of the cooled water entering the heat exchanger is assumed to be at (3^{o}C) higher than the ambient wet bulb temperature. The reference value of heat exchanger effectiveness was assumed 0.85.

The process air is then evaporatively cooled through a wet pad evaporative cooler before entering the greenhouse. The dry-bulb temperature of the process air leaving the evaporative cooler is:

$$T_{dbo} = T_{dbi} + \varepsilon_{ev}\left(T_{dbi} - T_{wbi}\right) \tag{31}$$

The value of evaporative cooler effectiveness was taken at 0.8.

5. OVERALL SYSTEM PERFORMANCE

The performance of open cycle desiccant cooling system is commonly expressed by two terms. The coefficient of performance (COP) and the cooling capacity (CC). Joudi and Madhi 1985 defined the COP as the heat removed from the process air stream divided by energy input to the cycle:

$$COP = \frac{\dot{m}_p(h_a - h_{sp})}{Energy\ input} \quad (32)$$

The energy input includes electric energy used to circulate air, water, and rotating the desiccant wheel, and auxiliary regeneration heat which is calculated as:

$$\text{Auxiliary energy} = \dot{m}_{reg}\, c_p\, (T_{reg} - T_o) \quad (33)$$

The cooling capacity of the process air supplied by the system is usually defined as the difference in enthalpy between the supply air and any given interior condition. Joudi and Madhi 1985 indicated that the sensible cooling capacity based on temperature difference is more factual than calculating it based on enthalpy difference. The cooling capacity of the current system was calculated as:

$$CC = \dot{m}_p\, c_p\, (T_r - T_{sp}) \quad (34)$$

6. RESULTS AND DISCUSSION

6.1 Factors Affecting Greenhouse Microclimate

A dynamic model was adopted, tested, and validated for a closed and properly sealed greenhouse. The ambient air temperature and incident solar radiation on a horizontal surface were used as input data to the model in order to predict the microclimate. **Fig. 3 a, b** shows the hourly variation of the predicted inside air and soil surface temperatures for typical winter and summer days. Both temperatures vary with the solar radiation intensity and reach maximum value about one hour after solar noon. The maximum inside air temperature in January was 36 ^{o}C at 1 p.m., while the minimum temperature was 3.5 ^{o}C at 6 a.m. Similarly, the maximum and minimum soil surface temperatures of the greenhouse were 45 ^{o}C and 5.5 ^{o}C at 1 p.m. and 6 a.m., respectively. In August, the maximum and minimum inside air temperatures were 82.5 ^{o}C and 30 ^{o}C. While, for the soil surface temperature it were 93.8 ^{o}C and 29 ^{o}C at 1 p.m. and 6 a.m., respectively. Clearly, the soil surface temperature is higher than the inside air temperature. This is due to the absorbed solar radiation by the soil, the storage effect of the soil, and the conducted heat from the warm ground to the soil surface.

The inside air temperature of the present model was compared with the sol-air temperature presented by Sethi and Sharma 2007 as shown in **Fig. 4 a, b.** The inside air temperature is seen higher than the sol-air temperature due to the soil heat gain which is included in the present model and not included in the sol-air temperature calculation. The two temperatures coincide during the night due to the diminished effect of the soil heat gain. The present dynamic model was further validated with the published results of the greenhouse simulator that was developed by Rodriguez et al. 2010 as shown in **Fig. 5.** Satisfactory agreement is noted for the inside air temperature with a maximum difference of 2.5 ^{o}C. While a large discrepancy of 5^{o}C is obtained for the soil surface temperature. Another verification was done with experimental results obtained by Kothari and Panwar 2007 as shown in **Fig. 6 a, b** and good agreement is observed.

The important parameters affecting the microclimate of the greenhouse are the ambient temperature, the intensity of solar radiation, and the ventilation rates. **Fig. 7a, b and Fig. 8a, b** show the variation of inside air and soil surface temperatures with ambient temperature at constant soil thermal conductivity, soil heat capacity, and solar radiation intensity at 12 noon, with various ventilation rates. As the ambient temperature increases, both the inside air and soil surface temperatures increase with almost a direct relationship. This is because an increase in the ambient temperature results in an increase in the heat transfer into the greenhouse at any ventilation rate. Also, it is evident that for a constant ambient temperature, an increase in the ventilation rate results in a decrease in both the inside air and soil surface temperatures.

The influence of ventilation rate on the inside to outside air temperature difference, keeping the soil physical properties and radiation intensity unchanged is shown in **Fig. 9** for January and August at 12 noon. As expected, an increase in the ventilation rate results in a decrease in the maximum greenhouse temperature. It is stipulated that air exchange rates between 0.75 and 1 change per minute, control effectively the temperature rise in a greenhouse (Ganguly and Ghosh 2009, Kittas et al. 2005).

The influence of outside solar radiation intensity on both the inside air and soil surface temperatures for constant soil properties, ambient temperature at 12 noon, and various ventilation rates for January and August is shown in **Fig. 10a, b and Fig. 11a, b** respectively. Such results have also been obtained by Ganguly and Ghosh 2009, and Kittas et al. 2005.

6.2 Factors Affecting Heating Load

The net heating load is obtained by subtracting the heat gains from heat losses. Heat loss from the greenhouse is mainly due to transmission and infiltration. Heat gains to the interior of the greenhouse are solar and soil heat gains. The solar radiation is the main heat gain component in greenhouses and the soil heat gain is the second major part. The results of the dynamic model (section 6.1) were used to determine the soil heat gain as shown in **Fig. 12**. The solar and soil heat gains counter balance the heat losses. As the heat loss exceeds the heat gain, a certain quantity of heat should be supplied. Whereas if the heat gain exceeds the heat loss, cooling by an appropriate method may be required. **Fig. 13** shows the total heating load estimated with maximum heating load at 6 a.m. at a value of about 198, 353,and 499 $W.m^{-2}$ in November, December, and January. However, if the inside air temperature obtained from the dynamic model is less than the design inside temperature of $20^{o}C$, heat should be supplied. Also, ventilation or evaporative cooling is sometimes required as shown in **Fig. 14**. A comparison between the present heat load calculation method and that presented by Mastalerz 1977, ASHRAE 1977, Aldrich and Bartok 1994 which discard the soil heat gain is shown in **Figs. 15 & 16.**

6.3 Factors Affecting Cooling Load

The sources of heat gain making up the cooling load of the greenhouse are external and internal. External sources comprise solar, transmission, and infiltration heat gains. The internal sources include mainly the soil heat gain which has not been included in any previous cooling or heating load calculation methods. **Fig. 17** illustrates the values of this gain. It can be noticed that there is no soil heat gain for the periods 10 p.m. to 8 a.m. This means zero or negative values of the difference between the soil surface and the inside air temperatures. No paper in the literatures surveyed had dealt with the cooling load estimation of a greenhouse. The papers cited base their estimations on experimental experience in evaporative cooling only.

The total cooling load and its individual components in July are depicted in **Fig. 18**. The hourly variation of the total cooling load for June, July, and August is shown in **Fig. 19**. The values are nearly the same for these months and all have the same trend. This is because the solar and the soil heat gains are similar in these months**.** The peak value of the cooling load which should be taken for design purposes occurs in August at a value of 1653 $W.m^{-2}$ of greenhouse floor area.

A comparison between the total cooling load of the present work and that obtained by the standard method (i.e, ASHRAE 1977, Aldrich and Bartok 1994, and Sethi and Sharma 2007) which discard the soil heat gain is shown in **Fig. 20 a, b**. Excellent agreement is observed between the present work and that of Aldrich and Bartok 1994, and Sethi and Sharma 2007. The cooling load of ASHRAE 1977 is shifted by about one hour to the right due to the storage effect of the cooling load temperature difference $CLTD$ and the cooling load factor CLF.

6.4 Solar Air Heater Performance

The solar air heater in the simulated system was used for heating the inlet air to the required temperature for the heating purpose in winter and for the regeneration of the desiccant material in summer. To achieve this aim, a combined parallel-series connection is used to achieve the required outlet air temperature and air flow rate. The variation of outlet air temperature for two collectors in series for the air mass flux of 0.06 $kg.s^{-1}.m^{-2}$ of collector area is shown in **Figs. 21 & 22**. The maximum outlet air temperature from this collector array is about $30^{o}C$ for January, which is suitable for the supply air temperature in the winter season. While, it is about $64^{o}C$ for August. When the required supply air temperature is not achieved by the solar collectors array, an auxiliary heater is required.

6.5 Solar Cooling System Performance

The influence of ambient temperature, ambient moisture content, regeneration temperatures, evaporative cooler effectiveness, heat exchanger effectiveness, and dehumidifier effectiveness on the performance of the desiccant

cooling system is evaluated in terms of supply air temperature, sensible cooling capacity and system coefficient of performance.

For poor, medium, and good dehumidifier performance with constant inlet ambient temperature and moisture content of the process air stream, increasing the regeneration air temperature markedly increases the reduction in process air moisture content. The reason is that the adsorption capacity of the silica gel increases. Also, the increase of regeneration temperature from 50 to 90^{o}C reduces the supply air temperature by 10.4%, 8.7%, and 7% for good, medium, and poor dehumidifier performance respectively. This is because the process air enters the evaporative cooler at a lower wet bulb temperature.

The important parameter in the evaluation of the desiccant cooling system is the sensible cooling capacity. The inside design condition is assumed at 28 ^{o}C dry bulb temperature and 70% relative humidity. Increasing the regeneration temperature from 50^{o}C to 90^{o}C results in an increase in the cooling capacity for good, medium, and poor dehumidifier performances respectively. Also, the present simulation results are in good agreement with the experimental values achieved by Joudi and Madhi 1985.

In evaluating the performance of the present desiccant cooling system, the desiccant dehumidifier was assumed to have a poor effectiveness of (0.2, 0.55) as indicated by Moneer 1997. The system was tested under ventilation and recirculation modes with a regeneration temperature of 65 ^{o}C for the recirculation mode, which can be achieved by the collector array and little auxiliary heating. The mass flow rate of the process air stream was set equal to 1.3 kg.s^{-1}, which is associated with the peak value of the cooling load of the greenhouse. The regeneration air stream was set equal to 0.858 kg.s^{-1} Thus, the ratio of the regeneration to the process air flow rate is 0.66.

The variation of the supply air temperature from the desiccant cooling system is shown in **Fig. 23 a, b**. It was found that the supply air temperature increases with the increase of the recirculation. This is because of the combined effect of the ambient temperature and the ambient moisture content.

Fig. 24 a, b shows the variation of the sensible cooling capacity of the desiccant cooling system operated in ventilation and recirculation modes in 17th August. The sensible cooling capacity is best at no recirculation.

The system COP during the simulated period of 17th August is shown in **Fig. 25** for recirculation mode of 20%. The maximum value of the COP of about 16 occurs at 1 p.m. with a regeneration temperature of 65 ^{o}C. This is attributed to the absence of auxiliary power input. The variation of the COP is due to the variation of the ambient conditions and the solar heated regeneration air temperature during the day. When the auxiliary heat source is used a lower coefficient of performance is obtained.

7. CONCLUSIONS

1. The inside air and soil surface temperatures reach their maximum values about one hour after solar noon, while the minimum occur at 6 a.m.
2. The solar, transmission, soil, and infiltration heat gains form about 45%, 29%, 25%, and 1% of the total cooling load, respectively.
3. Solar and the soil heat gains are the main heat gain components to the interior of the greenhouse in both winter and summer seasons.
4. The energy balance method which includes the soil heat gain for estimating the heating and cooling loads of the greenhouse is more accurate than the methods followed by Mastalerz 1977, ASHRAE 1977, Aldrich and Bartok 1994 and Sethi and Sharma 2007.
5. Excellent agreement was obtained between the present work and that of ASHRAE 1977, Aldrich and Bartok 1994, and Sethi and Sharma 2007 in calculating the cooling load when the soil heat gain was added to these methods.
6. Two collector rows give an air temperature of 30^{o}C and 64^{o}C at midday in January and August respectively at mass flux of 0,06 kg.s^{-1}.m^{-2} of collector area are suitable for heating and cooling.
7. The desiccant cooling system can supply air at temperature of 19.5 ^{o}C during 17th August for an operation mode of 20% recirculation and regeneration temperature of 65 ^{o}C for design condition of 28 ^{o}C and 70% relative humidity.

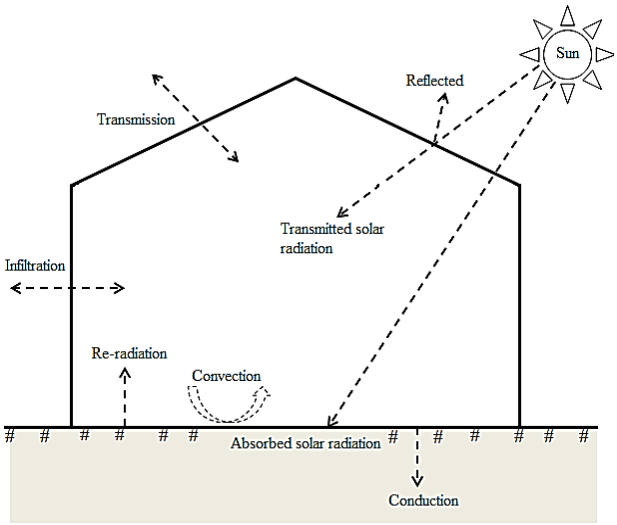

Fig. 1 The greenhouse under study and its heat exchanges with the surroundings.

Table 1 Constants used in greenhouse microclimate model.

Symbol	Value
ρ	1.2 kg/m^3
c_p	1010 J/kg.K
C_s	1980000 J/m^3.K
ϵ_s	0.9
α_s	0.8
z_o	0.5 m
z_b	0.45 m
T_b	15 ^{o}C
k_s	1.9 W/m.K
N	1.25 hr^{-1}
U	6.246 W/m^2.^{o}C
H	2.5 m
r	4.6642
σ	5.67*10^{-8} W/m^2.K

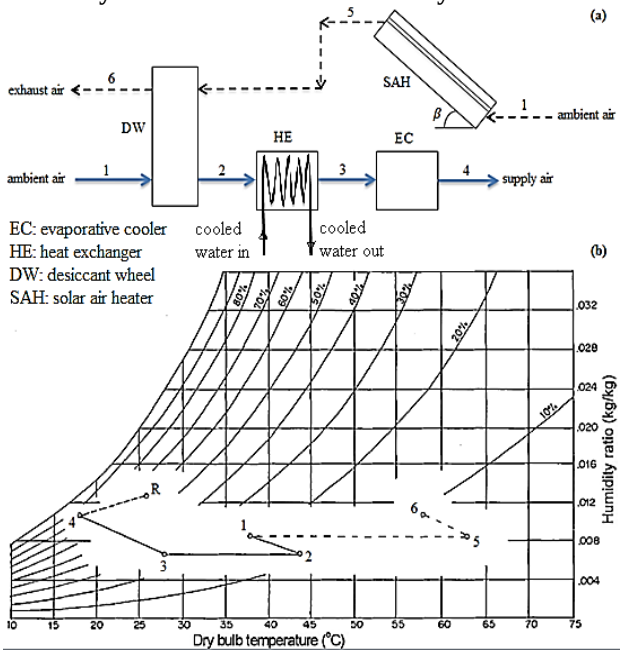

Fig. 2 (a) A schematic diagram of the simulated system; (b) Psychometric representation of the cycle.

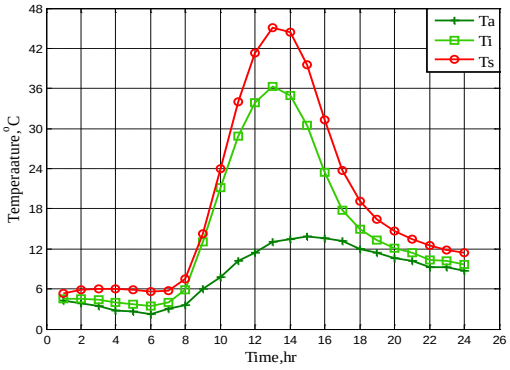

(a) 17th January.

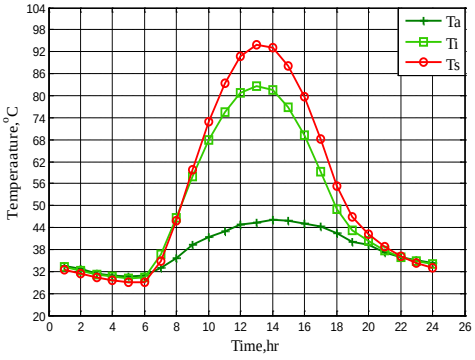

(b) 17th August.

Fig. 3 Hourly variation of ambient and the predicted inside air and soil surface temperatures for the greenhouse.

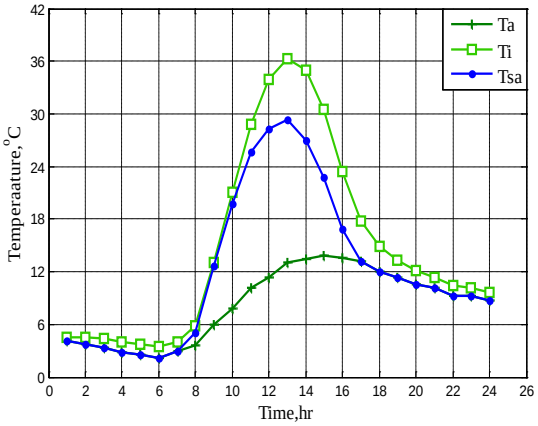

(a)17th January.

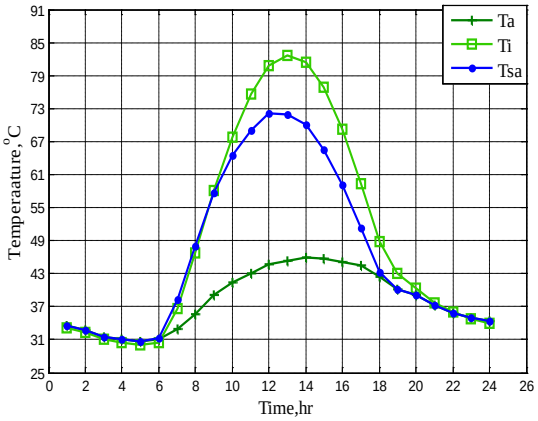

(b) 17th August.

Fig. 4 Variation of ambient air, inside air, and sol-air temperatures with time of day.

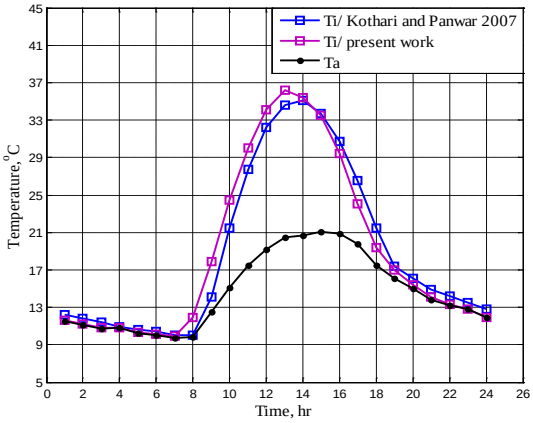

(a)

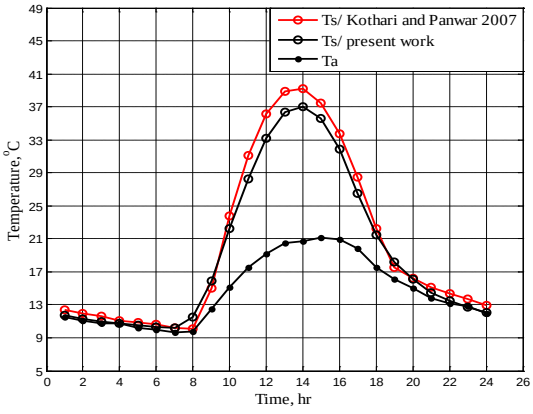

(b)

Fig. 6 Experimental and computer simulation results of (a) inside air temperature and (b) soil surface temperature through time of a winter day.

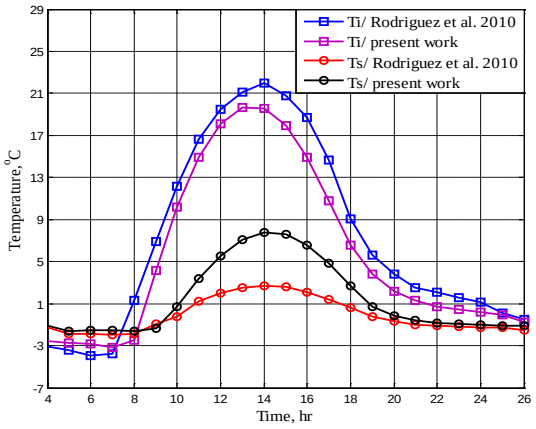

Fig. 5 Comparison between the results of the present simulation and Rodriguez et al. 2010 for a winter day.

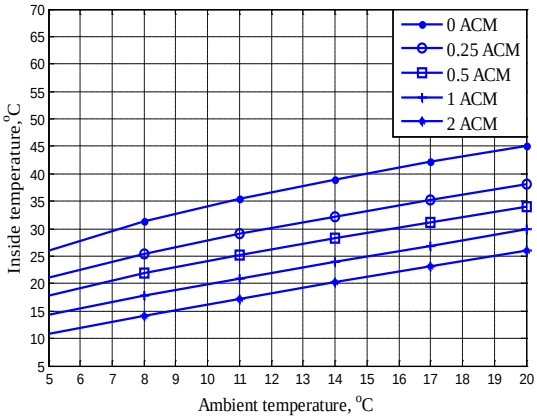

(a) 17th January.

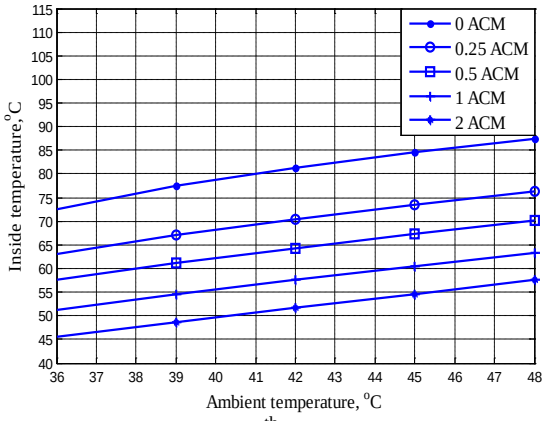

(b) 17th August.

Fig. 7 Variation of inside air temperature for various ventilation rates with ambient temperature.

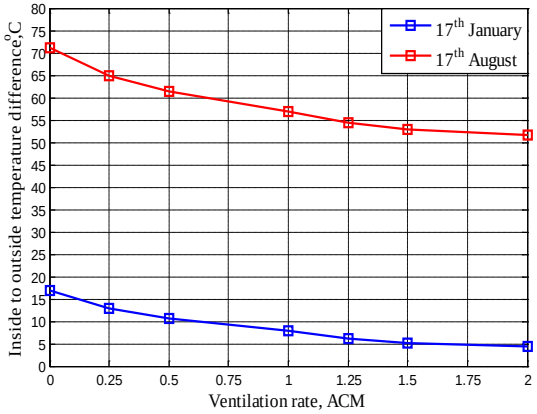

Fig. 9 Variation of inside to outside air temperature difference with ventilation rates for 17th January and 17thAugust.

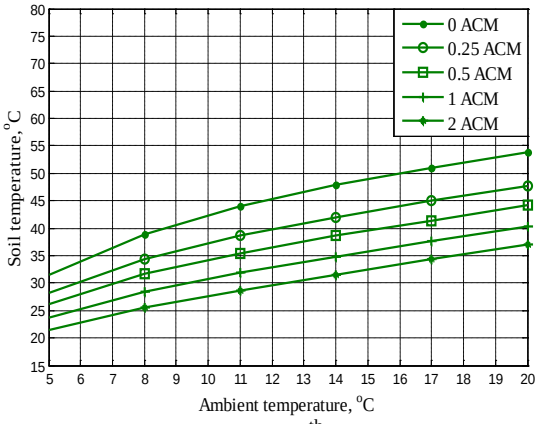

(a) 17th January.

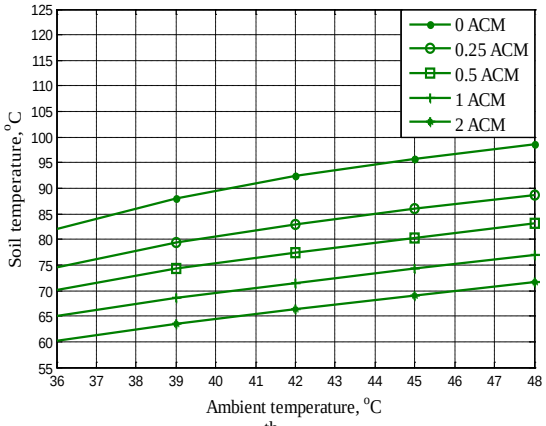

(b) 17th August.

Fig. 8 Variation of soil surface temperature for various ventilation rates with ambient temperature.

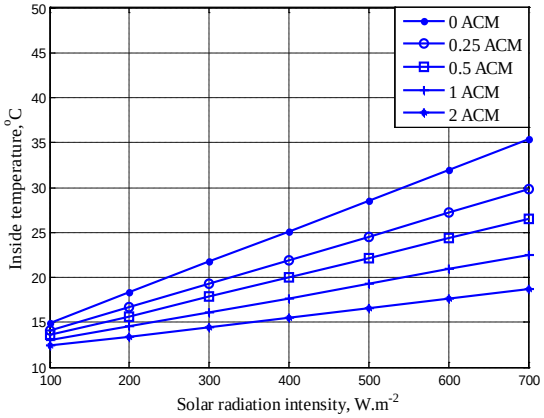

(a) 17th January.

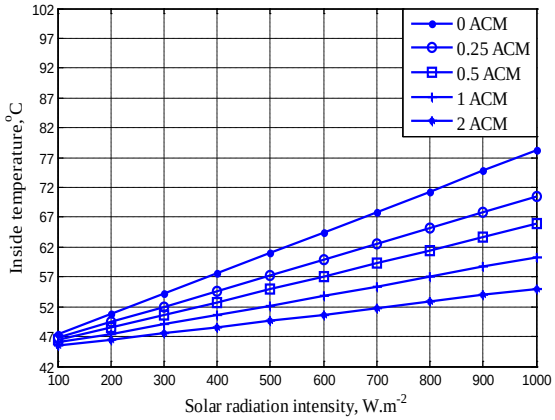

(b) 17th August.

Fig. 10 Influence of outside radiation intensity on the inside air temperature of the greenhouse for various ventilation rates.

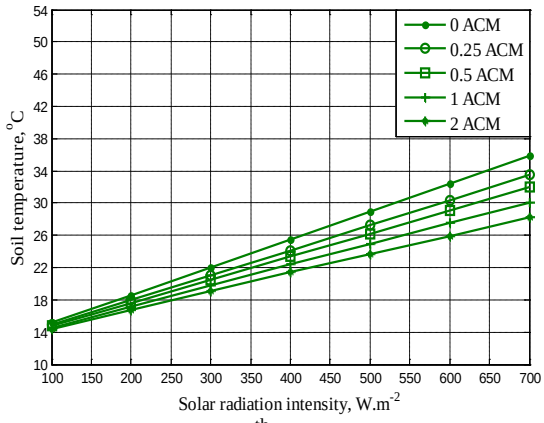

(a) 17th January.

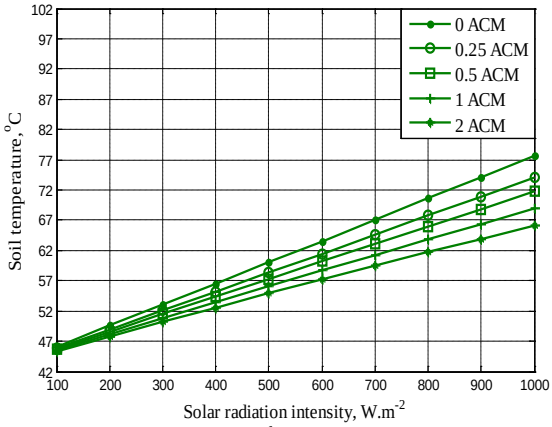

(b) 17th August.

Fig. 11 Influence of outside radiation intensity on the soil surface temperature of the greenhouse for various ventilation rates.

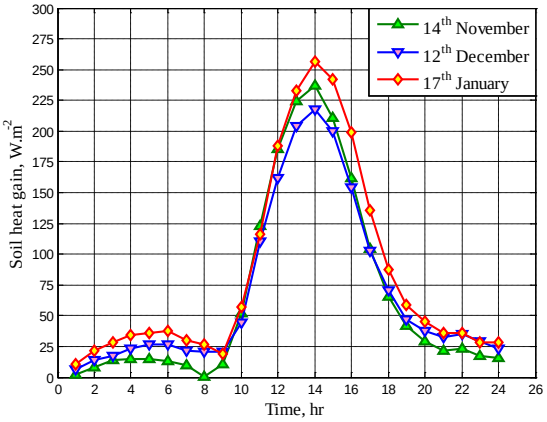

Fig. 12 Hourly variation of soil heat gain of the greenhouse.

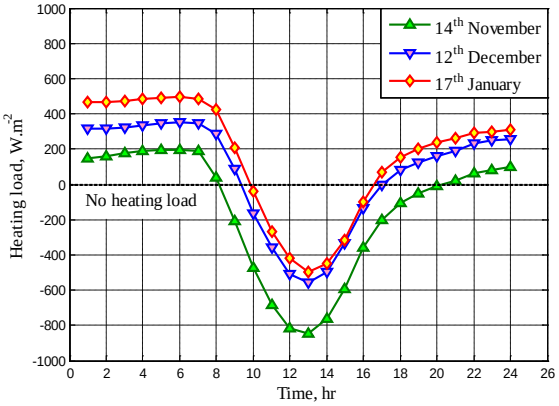

Fig. 13 Hourly variation of heating load of the greenhouse for typical winter days.

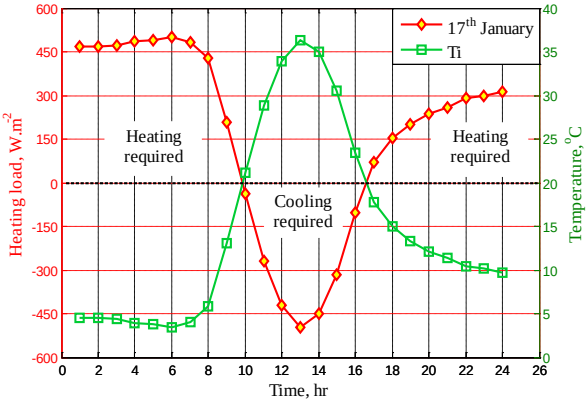

Fig. 14 Starting and ending time of the heating requirements.

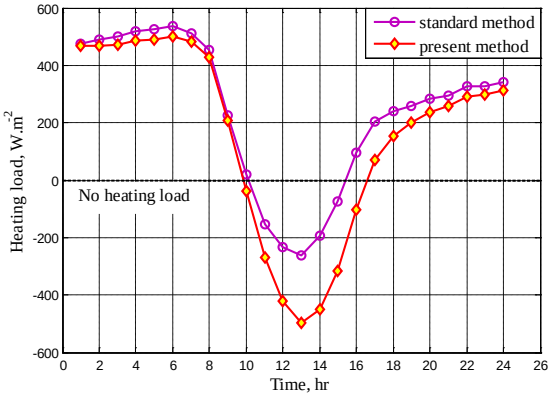

Fig. 15 The heating load estimated by the present and standard (i.e, Mastalerz 1977, ASHRAE 1977, Aldrich and Bartok 1994) methods.

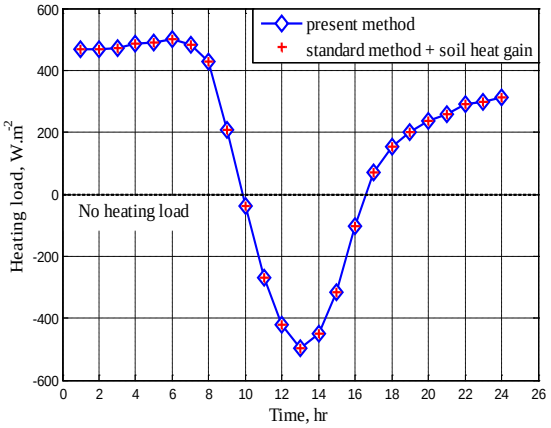

Fig. 16 The heating load estimated by the present and standard (i.e, Mastalerz 1977, ASHRAE 1977, Aldrich and Bartok 1994) methods. But adding the soil heat gain.

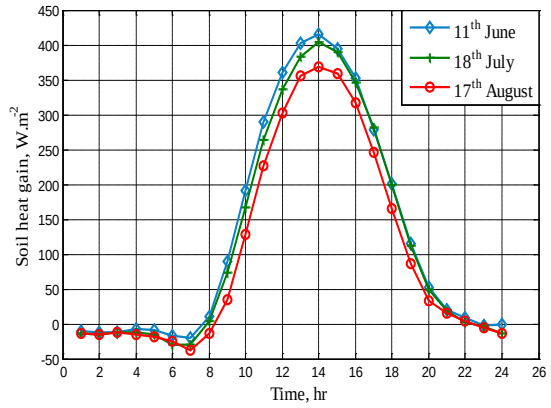

Fig. 17 Hourly variation of soil heat gain of the greenhouse.

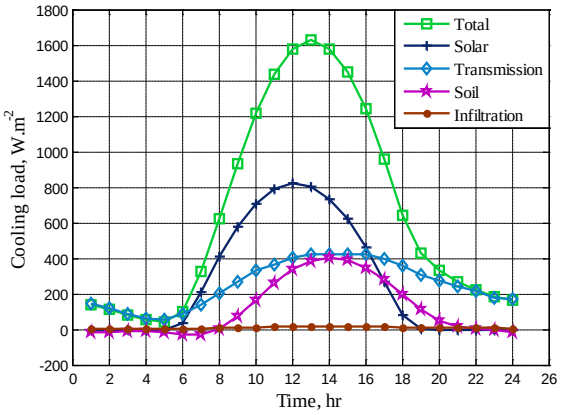

Fig. 18 Hourly variation of the total and various cooling load components in July.

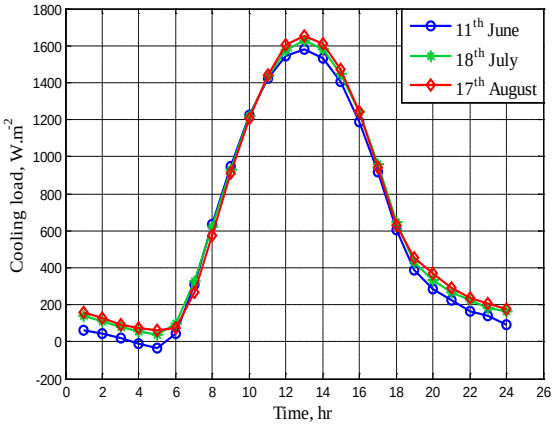

Fig. 19 Hourly variation of total cooling load in summer months.

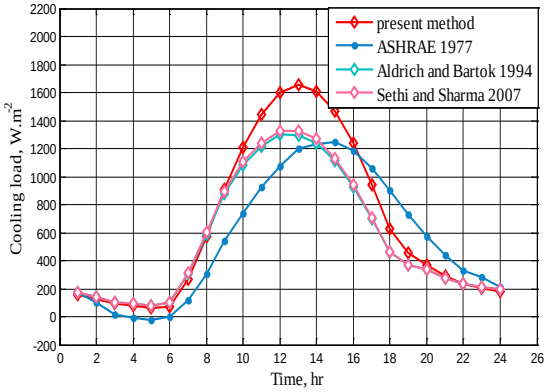

(a) Without soil heat gain.

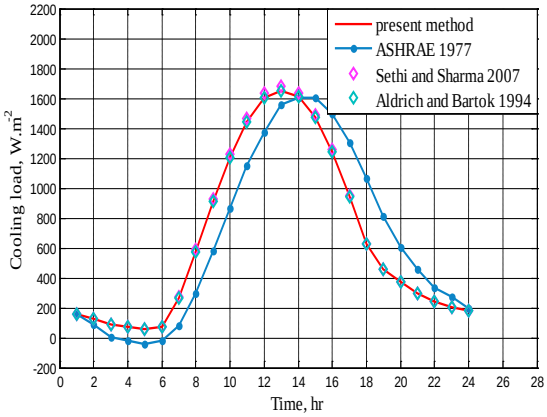

(b) With soil heat gain

Fig. 20 Comparison between the cooling loads estimated by the present and (ASHRAE 1977, Aldrich and Bartok 1994, and Sethi and Sharma 2007) methods.

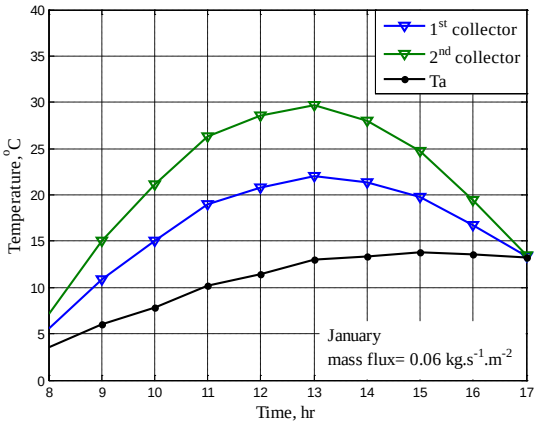

Fig. 21 Variation of outlet air temperature for two collectors in series in 17th January.

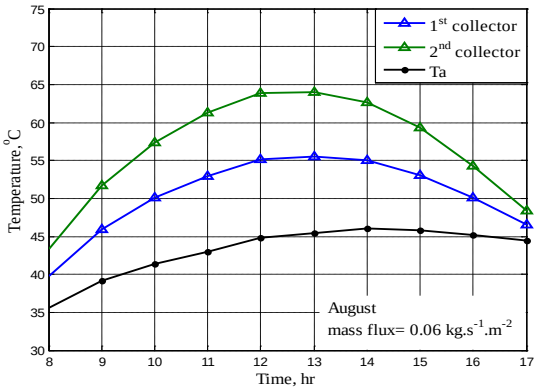

Fig. 22 Variation of outlet air temperature for two collectors in series in 17th August.

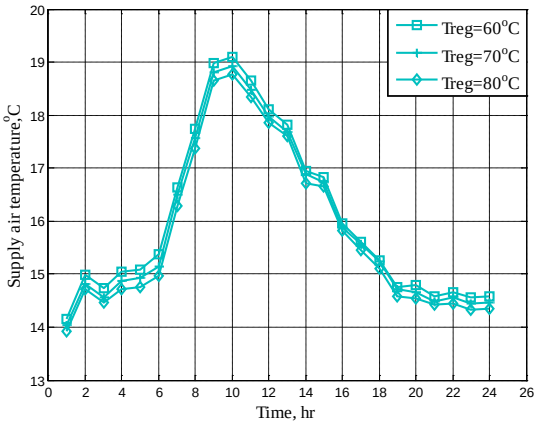

(a)

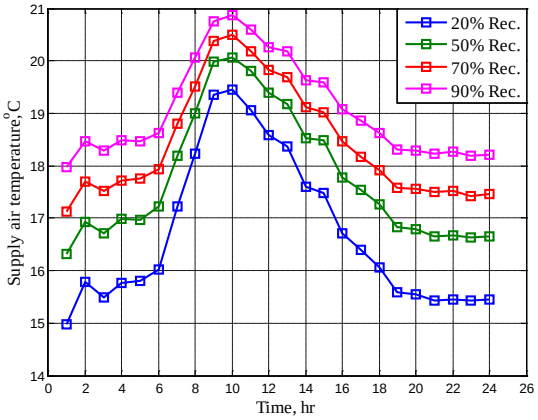

(b)

Fig. 23 Hourly variation of supply air temperature (a) for ventilation mode operation with varying regeneration temperature, (b) for various operation modes.

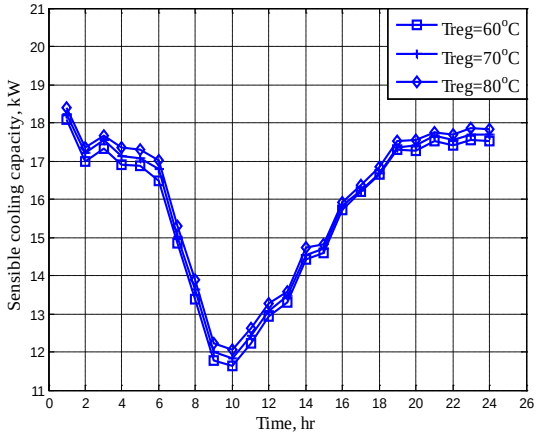

(a)

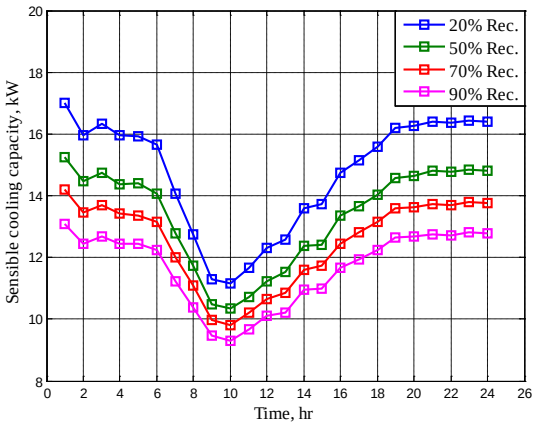

(b)

Fig. 24 Hourly variation of sensible cooling capacity (a) for ventilation mode operation with varying regeneration temperature, (b) for various operation modes.

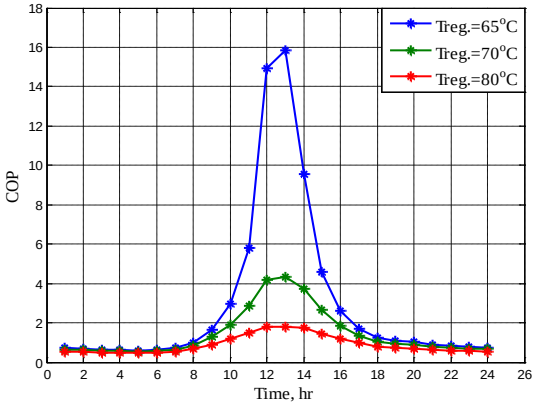

Fig. 25 Hourly variation of coefficient of performance for 20% return air with varying regeneration temperatures.

REFERENCES

Abdel-Ghany A.M. Solar energy conversions in the greenhouses. Sustainable Cities and Society 2011; 1: 219– 26.

Abdel-Ghany A.M., Al-Helal I.M. Solar energy utilization by a greenhouse: General relations. Renewable Energy 2011; 36:189-96.

Abdel-Ghany A.M., Kozai T. Cooling Efficiency of Fogging Systems for Greenhouses. Biosystems Engineering 2006; 94 (1): 97–109.

Aldrich R.A., Bartok J.W. Greenhouse Engineering. New York: Ithaca, 1994.

Amri-Alm A.M.S. Solar energy utilization in greenhouse tomato production. Journal of King Saud University, Agricultural Sciences 1997; 9: 21–38.

ASHRAE Handbook of Fundamental, American society for Heating, Refrigeration and Air Conditioning Engineers, Inc., New York,(1997).

Businger J.A. The glasshouse (greenhouse) climate. In Physical of Plant Environment 1963 (ed. By W.A. van Wijk).

Davies P.A. A solar cooling system for greenhouse food production in hot climates. Solar Energy 2005; 79 (6): 661–8.

Duffie J.A. and Beckman W.A., Solar Engineering and Thermal Process, John Wiley and Sons, New York, (2006).

Fong K.F., Chow T.T., Lin Z., Chan L.S. Simulation–optimization of solar-assisted desiccant cooling system for subtropical Hong Kong. Applied Thermal Engineering 2010; 30: 220–8.

Ganguly A., Ghosh S. Model development and experimental validation of a floriculture greenhouse under natural ventilation. Energy and Buildings 2009; 41: 521-7.

Hepbasli A. A comparative investigation of various greenhouse heating options using exergy analysis method. Applied Energy 2011; 88: 4411–23.

Jain D., Tiwari G.N. Modeling and optimal design of evaporative cooling system in controlled environment greenhouse, Energy Conversion and Management 2002; 43 (1):2235–50.

Joudi K.A., Dhaidan N.S. Application of solar assisted heating and desiccant cooling systems for a domestic building. Journal of Energy Conversion and Management 2001; 42:995-1022.

Joudi K.A., Madhi S.M. AN EXPERIMENTAL INVESTIGATION INTO A SOLAR ASSISTED DESICCANT EVAPORATIVE AIR CONDITIONING SYSTEM. Solar Energy 1987; 39 (2): 97-107.

Kano A., Sadler E.J. Survey of Greenhouse Models. J. Agr. Met. 1985; 41 (1): 75-81.

Kittas C., Karamanis M., Katsoulas N. Air temperature regime in a forced ventilated greenhouse with rose crop. Energy and Buildings 2005; 37 (8): 807–12.

Kothari S., Panwar N.L. Steady state thermal model for predicting micro-climate inside the greenhouse. Inst. Eng. (India) J. Agric. Eng. 2007; 88:52–5.

Kurklu A., Bilgin S., Ozkan B. A study on the solar energy storing rock-bed to heat a polyethylene tunnel type greenhouse. Renewable Energy 2003; 28 (5): 683–97.

Mastalerz J.W. The Greenhouse Environment. John Wiley and Sons, New York, 1977

Mesmoudi K., Soudani A., Zitouni B., Bournet P.E., Serir L. Experimental study of the energy balance of unheated greenhouse under hot and arid climates: Study for the night period of winter season. Journal of the Association of Arab Universities for Basic and Applied Sciences 2010; 9: 27–37.

Moneer A.K. A preliminary computer simulation of an open solar assisted desiccant cooling system, M.Sc. Thesis, university of Baghdad, Baghdad, (1997).

Rodriguez E.F., Kubota C., Giacomelli G.A., Tignor M.E., Wilson S.B., McMahon M. Dynamic modeling and simulation of greenhouse environments under several scenarios: A web-based application. Computers and Electronics in Agriculture 2010; 70: 105–16.

Roy J.C., Boulard T., Kittas C., Wang S. Convective and Ventilation Transfers in Greenhouses, Part 1: the Greenhouse considered as a Perfectly Stirred Tank. Biosystems Engineering 2002; 83 (1): 1–20.

Sethi V.P., Sharma S.K. Survey and evaluation of heating technologies for worldwide agricultural greenhouse applications. Solar Energy 2008; 82:832–59.

Sethi V.P., Sharma S.K. Thermal modeling of a greenhouse integrated to an aquifer coupled cavity flow heat exchanger system. Solar Energy 2007; 81:723–41.

Shukla A., Tiwari G.N., Sodha MS. Experimental study of effect of an inner thermal curtain in evaporative cooling system of cascade greenhouse. Solar Energy 2008; 82 (1):61–72.

Singh G., Singh P.P., Lubana P.P.S., Singh K.G. Formulation and validation of a mathematical model of the microclimate of a greenhouse. Renewable Energy 2006; 31: 1541–60.

White J.W., Aldrich R.A. Progress report on energy conservation for greenhouses research. Floriculture Review 1975; 156: 63-5.

NOMENCLATURE

A_c	Collector area (m^2)
$B1,2$	Iso potential lines of process and regeneration air streams
C	Volumetric heat capacity ($J/m^3.K$)
CC	Cooling capacity (W)
COP	Coefficient of performance
c_p	Specific heat of air (J/kg.K)
D_f	Collector dust factor
F_R	Heat removal factor
G	Air mass flow rate per unit area of collector ($kg/s.m^2$)
H	Average height of greenhouse (m)
h	Enthalpy of air/ Convection heat transfer coefficient
I	Incident solar radiation (W/m^2)
K	Thermal conductivity (W/m.K)
$\dot{m}$	Mass flow rate (kg/s)

N Number of air changes per hour (hr^{-1})

Q_u Useful energy gained from collector (W)

q_{co} Convection heat transfer rate between soil and inside air (W/m^2)

q_g Energy transferred from soil to inside air (W/m^2)

q_{inf} Infiltration heat transfer (W/m^2)

q_k Conduction heat transfer (W/m^2)

q_r Radiation heat transfer rate between soil and inside air (W/m^2)

q_{sg} Solar radiation absorbed within the Greenhouse (W/m^2)

q_{ss} Solar radiation absorbed within the soil (W/m^2)

q_t Transmission heat transfer (W/m^2)

r Ratio of glazing surface to soil surface area

S Absorbed solar radiation (W/m^2)

S_f Collector shade factor

SC Shading coefficient

$SHG_{max.}$ Maximum solar heat gain of window (W/m^2)

T Temperature (°C)

U Overall heat loss coefficient ($W/m^2.K$)

z_o Soil depth of layer 0 (m)

z_b Soil depth of layer b (m)

GREEK SYMBOLS

α_s Soil surface absorptivity of solar radiation

ε Effectiveness/ Emissivity

η Efficiency of collector

ρ Density of air (kg/m^3)

τ Transmittance

$\tau\alpha$ Transmittance-absorbtance product

σ Stefan-Boltzmann constant ($W/m.K^4$)

SUBSCRIPTS

a Ambient

b Beam

d Inside design/ Diffuse

db Dry bulb

ev Evaporative cooler

h Horizontal

hx Heat exchanger

i Inlet/ Inside

o Outlet

p Plate/ Process air

r Ground reflected/ Radiation/ Room

reg Regeneration air

s Soil

sa Sol-air

sp Supply air

t Total

w Water

wb Wet bulb

ABBREVIATIONS

ACCFHES Aquifer coupled cavity flow heat exchanger system

ACM Air change per minute

CLF Cooling load factor

$CLTD$ Cooling load temperature difference

EAHES Earth air heat exchanger system